Joint alignment of multiple protein-protein interaction networks via convex optimization

Hashemifar, Somaye
hashemifar@ttic.edu

Huang, Qixing
huangqx@ttic.edu

Xu, Jinbo
j3xu@ttic.edu

arXiv:1604.03482v1 [cs.DS] 12 Apr 2016

Abstract.
Motivation: High-throughput experimental techniques have been producing more and more protein-protein interaction (PPI) data. PPI network alignment greatly benefits the understanding of evolutionary relationship among species, helps identify conserved sub-networks and provides extra information for functional annotations. Although a few methods have been developed for multiple PPI network alignment, the alignment quality is still far away from perfect and thus, new network alignment methods are needed.
Result: In this paper, we present a novel method, denoted as ConvexAlign, for joint alignment of multiple PPI networks by convex optimization of a scoring function composed of sequence similarity, topological score and interaction conservation score. In contrast to existing methods that generate multiple alignments in a greedy or progressive manner, our convex method optimizes alignments globally and enforces consistency among all pairwise alignments, resulting in much better alignment quality. Tested on both synthetic and real data, our experimental results show that ConvexAlign outperforms several popular methods in producing functionally coherent alignments. ConvexAlign even has a larger advantage over the others in aligning real PPI networks. ConvexAlign also finds a few conserved complexes among 5 species which cannot be detected by the other methods.

1 Introduction

Protein-protein interaction (PPI) networks provide valuable information for understanding of protein functions and system-level cellular processes. The alignment of PPI networks is a useful means for comparing the networks of different species. This comparison helps identify evolutionarily conserved pathways/complexes that may be functionally significant. Studying the conserved modules may provide useful information about the molecular mechanism contributing to their functions.

PPI networks can be aligned either locally or globally. Local network alignment methods such as Mawish [12] and AlignNemo [2] aim to find small isomorphic subnetworks. Global network alignment (GNA) methods maximize the overall match between input networks. Some GNA methods such as IsoRank [26,27], MI-GRAAL [13], GHOST [19], MAGNA [23, 32], Prob [30], NETAL [18] and HubAlign [5] are designed for pairwise alignment, while others such as IsoRankN [15] and NetCoffee [6] for multiple alignment. GNA can be one-to-one or many-to-many mapping. The latter allows one protein to be aligned to multiple proteins of a single network while the former does not.

More attention has been paid to pairwise network alignment. With the availability of more PPI networks, it becomes inevitable to align multiple networks. Existing GNA methods such as NetworkBlast-M [9, 25] and GraemLin 2.0 [3] are designed for local alignment of multiple networks, whereas others such as IsoRankN [15], SMETANA [22], NetCoffee [6], BEAMS [1] and FUSE [4] for global alignment of multiple networks. In addition to sequence similarity, all these methods excluding NetworkBlast-M and NetCoffee also employs topological information. Moreover, all the methods except NetCoffee are designed for

many-to-many alignments. NetworkBlast-M starts with a set of highly conserved regions and then extends them greedily. GraemLin2.0 integrates phylogenetic information and network topology and then employs a hill-climbing algorithm to generate the alignment. IsoRankN applies IsoRank to compute the alignment scores between each pair of networks and then uses a PageRank-Nibble algorithm to cluster the proteins. SMETANA employs a semi-Markov random walk model to measure similarity between proteins. BEAMS constructs a weighted k-partite graph in which edges are assigned weights derived from protein sequence similarity. NetCoffee applies a triplet approach similar to T-Coffee to compute the edge weights of the k-partite graph. Both BEAMS and NetCoffee apply a heuristic on the k-partite graph to build an alignment. BEAMS fulfills this by greedily merging a set of disjoint cliques while NetCoffee by applying a simulated annealing method on a set of candidates. FUSE applies a non-negative matrix tri-factorization method to compute edge weights of the k-partite graph.

Most of existing GNA methods do not optimize alignment of all proteins simultaneously. Instead, they start from the best alignment between a subset of proteins and then gradually extend it by adding more proteins using a greedy strategy. This may impact alignment quality since errors introduced at an earlier stage cannot be fixed later.

This paper presents a novel one-to-one GNA algorithm, denoted as ConvexAlign, to align multiple PPI networks using a new scoring scheme that integrates network topology, sequence similarity and interaction conservation score. It is NP-hard to optimize such a scoring function. We formulate this GNA problem as an integer program and relax it to a convex optimization problem, which enables us to simultaneously align all the PPI networks, without resorting to the widely-used seed-and-extension or progressive alignment methods. Then we use an ADMM (alternating direction method of multipliers) method (see `http://stanford.edu/~boyd/admm.html`) to solve the relaxed convex optimization problem and optimize all the protein mappings together. Tested on the PPI networks of five different species, ConvexAlign outperforms several popular methods such as IsoRankN, SMETANA, NetCoffee and BEAMS in terms of biological alignment quality. ConvexAlign finds a few conserved complexes among these 5 species which cannot be found by the other methods. ConvexAlign also performs very well in aligning some publicly available synthetic networks.

2 Method

Definition. We represent a protein-protein interaction network by an undirected graph $G = (V, E)$ where V is the set of vertices (proteins) and E the set of edges (interactions). Let $d(u)$ denote the degree of vertex u and $e = (u, v) \in E$ represent an edge. A one-to-one global alignment $\mathcal{A}$ between N networks $G_i = (V_i, E_i), 1 \leq i \leq N$, is given by a decomposition of all nodes $\mathcal{V} = \cup_{i=1}^{N} V_i$ such that $\mathcal{V} = \mathcal{A}_1 \cup \cdots \cup \mathcal{A}_K$ where each $\mathcal{A}_i$ contains at most one protein from each network and any two $\mathcal{A}_i$ and $\mathcal{A}_j$ are disjoint. We call each A_i in the alignment a group or a cluster. Proteins in each cluster are mutually aligned to one another.

2.1 Scoring function for network alignment

Our goal is to find an alignment that maximizes the number of preserved edges and the number of *matched* orthologous (or functionally conserved) proteins. For this purpose we use a node score for scoring *matched* proteins and an edge score for scoring *matched* interactions, respectively. For a pair of proteins, their node score is the combination of their topology score and sequence similarity score. We use a minimum-degree heuristic algorithm to calculate the topological score, which was used by us to develop a pairwise GNA method HubAlign [5]. A recent third-party evaluation by Pržulj group [16] has shown that this topological score works very well in pairwise GNA. Please see our paper [5] for more details. We use the normalized BLAST bit scores for sequence similarity. Let $B(v_i, v_j)$ and $T(v_i, v_j)$ respectively denote the sequence sim-

ilarity and topology score between a pair of proteins $v_i \in V_i$ and $v_j \in V_j$. Then the node score $\text{node}(v_i, v_j)$ is calculated as follows:

$$\text{node}(v_i, v_j) = (1 - \lambda_1)\text{B}(v_i, v_j) + \lambda_1 \text{T}(v_i, v_j), \tag{1}$$

where λ_1 controls the importance of the topology score relative to the BLAST score. The node score of multiple alignment $\mathcal{A}$, i.e. $f_{node}(\mathcal{A})$, sums the scores among all pairs of *matched* proteins:

$$f_{node}(\mathcal{A}) = \sum_{1 \le i < j \le N} \sum_{\mathcal{A}_k \in \mathcal{A}, v_i, v_j \in \mathcal{A}_k} \text{node}(v_i, v_j). \tag{2}$$

The edge score $f_{interaction}(A)$ measures interaction-preserving in an alignment $\mathcal{A}$. This score counts the number of interactions aligned between all pairs of networks:

$$f_{interaction}(\mathcal{A}) = \sum_{1 \le i < j \le N} \sum_{\mathcal{A}_k, \mathcal{A}_l \in \mathcal{A}, v_i, v_j \in \mathcal{A}_k, v_i', v_j' \in \mathcal{A}_l} \delta((v_i, v_i') \in E_i)\delta((v_j, v_j') \in E_j), \tag{3}$$

where $\delta((v_i, v_i') \in E_i)$ is an indicator function. We aim to find the multiple alignment $\mathcal{A}$ that maximizes a combination of node and interaction scores as follows.

$$f = (1 - \lambda_2) f_{node}(\mathcal{A}) + \lambda_2 f_{interaction}(\mathcal{A}), \tag{4}$$

where λ_2 describes the tradeoff. See Appendix for determination of λ_1 and λ_2 by cross-validation.

2.2 Integer and Convex Programming Formulation

Definition. A one-to-one multiple network alignment is valid or feasible if the following condition (also called consistency property) is satisfied: for any three vertices v_i, v_j, and v_k of three different networks, if v_i is aligned to v_j and v_j aligned to v_k, then v_i is aligned to v_k.

Parameterizing multiple alignments. Let M be the number of proteins in all the input PPI networks i.e. $M = \sum_{i=1}^{N} |V_i|$. We may represent a valid multiple alignment $\mathcal{A}$ by a binary matrix $Y = (Y_1; Y_2; \cdots; Y_N) \in \{0, 1\}^{M \times K}$, where each block Y_i encodes the association between V_i and $\mathcal{A}$. Each row of Y corresponds to one vertex and each column to one alignment cluster. That is, $\forall v_i \in V_i, Y_i(v_i, A_j) = 1$ if and only if v_i is in cluster A_j. Let $\mathbf{1}$ be a vector of appropriate size with all elements being 1. Since Y is a one-to-one alignment, it shall satisfy the following constraints:

- Each row of Y has exactly one non-zero entry, i.e., $Y\mathbf{1} = \mathbf{1}$.
- Each column of Y has at most N non-zero entries, i.e., $Y^T\mathbf{1} \le N\mathbf{1}$.
- Each column of Y_i has at most one non-zero entry, i.e., $Y_i^T\mathbf{1} \le \mathbf{1}$.

On the other direction, any binary matrix Y satisfying the above properties encodes a one-to-one alignment.

Although Y is a good representation of an MNA, the objective function with Y as variable is nonlinear and thus, hard to optimize. Inspired by [7], we introduce another alignment matrix X as follows.

$$X = \begin{pmatrix} I_{|V_1|} & X_{12} & \cdots & X_{1N} \\ X_{12}^T & I_{|V_2|} & \cdots & X_{2N} \\ \vdots & \cdots & \ddots & \vdots \\ X_{1N}^T & \cdots & \cdots & I_{|V_N|} \end{pmatrix} = \begin{pmatrix} Y_1 \\ Y_2 \\ \vdots \\ Y_N \end{pmatrix} \cdot \begin{pmatrix} Y_1^T & Y_2^T & \cdots & Y_N^T \end{pmatrix}, \tag{5}$$

where each block $X_{ij} = Y_i Y_j^T$ is a binary matrix encoding the mapping between V_i and V_j. That is, $X_{i,j}(v_i, v_j) = 1$ if and only if v_i and v_j are aligned (i.e., in the same alignment cluster).

It is easy to see that X is positive semi-definite. Since this section considers only one-to-one mapping, for any two i and j ($i \neq j$), each row or column of X_{ij} has at most one non-zero element, i.e., $X_{ij}\mathbf{1} \leq \mathbf{1}$ and $X_{ij}^T\mathbf{1} \leq \mathbf{1}$ where $\mathbf{1}$ is a vector of appropriate size with all entries 1. On the other direction, we have the following proposition (see Appendix D for its proof).

Proposition 1. *Let X be a binary block matrix with $N \times N$ blocks, and X_{ij} be the block in the i^{th} row and the j^{th} column. If X satisfies the following conditions: (1) $X \succeq 0$, (2)$X_{ii} = I_{|V_i|}$ for $1 \leq i \leq N$, and (3)$X_{ij}\mathbf{1} \leq \mathbf{1}$ and $X_{ij}^T\mathbf{1} \leq \mathbf{1}$ for $1 \leq i < j \leq N$, then X encodes a feasible global alignment of N networks admitting one-to-one mapping and satisfying the cycle consistency property.*

Therefore, we may encode a one-to-one GNA using X, which leads to a linear formulation of the objective function. Following Prop. 1, we impose the following constraints on X:

$$\begin{aligned} X_{ij}\mathbf{1} \leq \mathbf{1},\ X_{ij}^T\mathbf{1} \leq \mathbf{1}, X_{ij} \in \{0,1\}^{|V_i|\times|V_j|} \qquad & (1 \leq i < j \leq N) \\ X \succeq 0, \qquad X_{ii} = I_{|V_i|} \qquad & (1 \leq i \leq N) \end{aligned} \tag{6}$$

Objective function. As X_{ij} is the indicator submatrix for V_i and V_j, the node score can be formulated as follows.

$$f_{node} = \sum_{1\leq i<j\leq N} \sum_{v\in V_i, v'\in V_j} \text{node}(v, v') X_{ij}(v, v') = \sum_{1\leq i<j\leq N} \langle C_{ij}, X_{ij}\rangle, \tag{7}$$

where C_{ij} is a matrix composed of the values of node(v, v').

To formulate $f_{interaction}$, we introduce indicator variables $y_{ij}(v_i, v_j, v_i', v_j')$ for edge correspondences:

$$y_{ij}(v_i, v_j, v_i', v_j') = X_{ij}(v_i, v_j) X_{ij}(v_i', v_j'), \quad \forall (v_i, v_i') \in E_i, (v_j, v_j') \in E_j, 1 \leq i < j \leq N. \tag{8}$$

$$f_{interaction} = \sum_{1\leq i<j\leq N} \sum_{(v_i,v_i')\in E_i, (v_j,v_j')\in E_j} y_{ij}(v_i, v_j, v_i', v_j') = \sum_{1\leq i<j\leq N} \langle \mathbf{1}, \boldsymbol{y}_{ij}\rangle, \tag{9}$$

where $\boldsymbol{y}_{ij}$ stacks the indicator variables between V_i and V_j.

The nonlinear constraint (8) can be replaced by the following linear inequalities (c.f. [8, 14]):

$$\begin{aligned} \forall v_j' \in V_j, \sum_{v_i':(v_i,v_i')\in E_i} y(v_i, v_j, v_i', v_j') \leq X_{ij}(v_i, v_j) \\ \forall v_i' \in V_i, \sum_{v_j':(v_j,v_j')\in E_j} y(v_i, v_j, v_i', v_j') \leq X_{ij}(v_i, v_j) \\ \forall v_j \in V_j, \sum_{v_i:(v_i,v_i')\in E_i} y(v_i, v_j, v_i', v_j') \leq X_{ij}(v_i', v_j') \\ \forall v_i \in V_i, \sum_{v_j:(v_j,v_j')\in E_j} y(v_i, v_j, v_i', v_j') \leq X_{ij}(v_i', v_j') \end{aligned} \tag{10}$$

It is easy to prove that (8) implies (10). On the other direction, considering that the coefficients of $\boldsymbol{y}$ is positive and we want to maximize (9), we shall be able to prove that (10) implies (8). We replace (8) by (10) to obtain linear constraints and summarize (10) in the matrix form as follows.

$$B_{ij}\boldsymbol{y}_{ij} \leq \mathcal{F}_{ij}(X_{ij}), \tag{11}$$

where B_{ij} is coefficient and $\mathcal{F}_{ij}$ is a linear operator that picks the corresponding element of X_{ij} for each constraint. That is, $\mathcal{F}_{ij}(X_{ij}(v_i, v_j)) =< P_{ij}, X_{ij} >$ where P_{ij} is a binary matrix with the same dimension as X_{ij} and only one element $P_{ij}(v_i, v_j)$ is equal to 1.

Finally, by integrating (7), (9), (11) and Prop. 1, we have the following integer program:

$$\begin{aligned}
\text{maximize} \quad & \sum_{1\le i<j\le N} \Big((1-\lambda_2)\langle C_{ij}, X_{ij}\rangle + \lambda_2 \langle \mathbf{1}, \mathbf{y}_{ij}\rangle\Big) \\
\text{subject to} \quad & \boldsymbol{y}_{ij} \in \{0,1\}^{|E_i|\times|E_j|},\ B_{ij}\boldsymbol{y}_{ij} \le \mathcal{F}_{ij}(X_{ij}), && 1 \le i < j \le N \\
& X_{ij}\mathbf{1} \le \mathbf{1},\ X_{ij}^T\mathbf{1} \le \mathbf{1}, X_{ij} \in \{0,1\}^{|V_i|\times|V_j|}, && 1 \le i < j \le N \\
& X \succeq 0, \quad X_{ii} = I_{|V_i|}, \quad 1 \le i \le N && (12)
\end{aligned}$$

The key constraint is $X \succeq 0$, which enforces cycle consistency in the alignments. $X \succeq 0$ still holds even $N = 2$.

2.3 Optimization via Convex Relaxation

It is NP-hard to directly optimizing (12) since the variables are binary. We may first relax them to obtain a convex optimization problem that can be solved to global optimum within polynomial time, and then employ a greedy rounding scheme to convert fractional solution to integral.

Convex relaxation. By relaxing $\boldsymbol{y}_{ij}$ and X_{ij} to real values between 0 and 1, we have the following convex program:

$$\begin{aligned}
\text{maximize} \quad & \sum_{1\le i<j\le N} \Big((1-\lambda_2)\langle C_{ij}, X_{ij}\rangle + \lambda_2 \langle \mathbf{1}, \mathbf{y}_{ij}\rangle\Big) \\
\text{subject to} \quad & \boldsymbol{y}_{ij} \ge \mathbf{0},\ B_{ij}\boldsymbol{y}_{ij} \le \mathcal{F}_{ij}(X), && 1 \le i < j \le N \\
& X_{ij}\mathbf{1} \le \mathbf{1},\ X_{ij}^T\mathbf{1} \le \mathbf{1},\ X_{ij} \ge 0, && 1 \le i < j \le N \\
& X \succeq 0, \quad X_{ii} = I_{|V_i|}, && 1 \le i \le N \qquad (13)
\end{aligned}$$

Optimization strategy. We use ADMM (alternating direction of multiplier method) to solve the convex relaxation (13). The basic idea is to augment its Lagrangian dual(see `https://en.wikipedia.org/wiki/Augmented_Lagrangian_method`) and iteratively optimize a subset of variables while keeping the others fixed. This allows us to exploit structure patterns in the constraint set for effective optimization. As the derivation is quite technical, we leave the details in Appendix E.

Rounding into an integer solution. The above convex relaxation has a pretty tight fractional solution. We propose a greedy rounding strategy to convert fractional solution to integral. We collect all the protein pairs with an indicator value $X(u, v) > 0.05$ and place them in a decreasing order into a sorted list $\mathcal{X}$. Then we build an alignment graph starting with an empty edge set by scanning through $\mathcal{X}$. For each scanned protein pair (u, v) in $\mathcal{X}$, in the alignment graph we add an edge to connect this pair as long as such an addition does not violate the constraint that no protein in one network is aligned to two proteins in another network. After all pairs are scanned, we decompose the alignment graph into connected components, each corresponding to a cluster of mutually-aligned proteins. The set of all the clusters form an alignment. Most components are cliques. For the very few non-clique components, we just add some edges to make them cliques.

3 RESULTS

We compare our algorithm ConvexAlign with several popular and publicly available methods IsoRankN [15], SMETANA [22], NetCoffee [6] and BEAMS [1]. We ran SMETANA and NetCofee with their default pa-

rameters. For both BEAMS and IsoRankN, we set three different values for their parameter $\alpha = \{0.3, 0.5, 0.7\}$. We left other parameters of BEAMS at their default values.

3.1 Test data

We use the PPI networks of H.sapiens (human), S.cerevisiae (yeast), Drosophila melanogaster (fly), Caenorhabditis elegans (worm) and Mus musculus (mouse) taken from IntAct [10]. The human network has 9003 proteins and 34935 interactions, the yeast network has 5674 proteins and 49830 interactions, the fly networks has 8374 nodes and 25611 interactions, the mouse network has 2897 proteins and 4372 interactions and the worm network has 4305 proteins and 7747 interactions. Only experimentally-validated PPIs are used.

We also use the NAPAbench [21] synthetic PPI networks. NAPAbench is a benchmark that contains PPI network families generated by three different network models: crystal growth(CG) [11], duplication-mutation-complementation(DMC) [31] and duplication with random mutation(DMR) [28]. We use the 8-way alignment dataset of this benchmark, which contains three network families each with 8 networks of 1000 nodes generated by one of the three network models. The 8-way alignment dataset simulates a network family of closely-related species, so this benchmark has very different properties as the above 5 real PPI networks. NAPAbench has recently been used to benchmark SMETANA.

3.2 Alignment quality measures

We evaluate multiple network alignment quality using several topological and functional consistency metrics proposed in different studies. Functional consistency measures however, are more important than topological measures since one of the important applications of network alignment is to functional annotation transfer. For topological analysis of the output clusters we use the following metrics.

c-coverage: It is the number of clusters composed of proteins from exactly c species. Specifically, total coverage is the number of clusters composed of proteins from at least two species. Clusters with large c explain a larger amount of data better than clusters with small c.

Conserved Interaction(CI): It is calculated as the ratio of the number of aligned interactions to the total number of interactions between output clusters.

A multiple alignment with a higher c-coverage (or total coverage) or CI is not necessarily biologically meaningful since it may align many unrelated proteins together. Therefore, we also employ GO terms to measure functional consistency or biological quality of an alignment. GO terms describe roles of proteins in terms of their associated biological process (BP), molecular function (MF) and cellular component (CC). We exclude root GO terms from analysis, i.e., GO terms on level higher than 5. We also exclude CC because proteins with matched CC are not usually considered functionally similar. Moreover, CC only annotates a small percentage of the proteins. The following measures are based on the observation that functionally related proteins are more likely to have similar GO terms.

Specificity: We say a cluster $annotated$ if at least two of its proteins have GO annotations. An annotated cluster is $consistent$ if all of its proteins share at least one common GO term. Specificity is defined as the ratio of consistent clusters to annotated clusters.

Average of functional similarity ($\overline{AFS}$). This score is based on the semantic similarity of the GO terms, which is derived from their distance in the ontology. We use Schlicker's similarity, based on the Resnik ontological similarity, to calculate the functional similarity in the BP and MF category [24]. Schlicker's similarity is one of the best performing methods for computing the functional similarity between proteins (see Appendix B for more details) [20]. Let $s_{cat}(u, v)$ denote the GO functional similarity of proteins u and v in category cat (i.e. BP or MF). AFS of an output cluster $\mathcal{A}$ in category cat is defined as follows:

$$AFS_{cat}(\mathcal{A}) = \frac{1}{\frac{|\mathcal{A}|\times(|\mathcal{A}|-1)}{2}} \sum_{v_i, v_j \in \mathcal{A}, i \neq j} s_{cat}(v_i, v_j)$$

Finally we define $\overline{AFS}$ in category cat as the average of AFS over all clusters. Following [6], we take into consideration all the clusters that contain at least 60% GO-annotated proteins to avoid ignoring many functionally meaningful clusters. We separately compare the $\overline{AFS}$ for clusters for $c = 3, 4, 5$. We also provide the distribution of the AFS scores for each given c.

Mean normalized entropy (MNE). The normalized entropy of a cluster $\mathcal{A}$ is defined as: $NE(\mathcal{A}) = \frac{1}{\log(d)} \times \sum_{i=1}^{d} p_i \times \log(p_i)$ where d is the number of different GO annotations in $\mathcal{A}$ and p_i represents the fraction of proteins in $\mathcal{A}$ with annotation GO_i. A cluster with lower entropy is more functionally coherent. MNE is the mean of normalized entropy over all annotated clusters.

Conserved orthologous interactions(COI): Similar to SMETANA, COI is calculated as the total number of interactions between all consistent clusters. COI may be a better measure than CI because it detects whether the conserved interactions are spurious or actually correspond to real conserved interactions between orthologous proteins. An alignment with larger COI may lead to identifying functionally conserved subnetwroks (i.e clusters) composed of orthologous genes.

Sensitivity: The closest cluster of a given GO term is the cluster that contains the maximum number of proteins associated with that GO term. Similar to BEAMS [1], we define Sensitivity as the average (over all GO terms) of the fraction of proteins in the closest cluster, that are associated with that GO term.

3.3 Alignment quality on real data

Topological quality. Table 1 lists the topological evaluation of the alignments produced by different methods. The first four multi-rows show the results for the clusters consisting of proteins belonging to $c = 2, 3, 4, 5$ species, respectively. In each multi-row, the top and bottom rows show c-coverage and the number of proteins in the clusters, respectively. ConvexAlign has a larger c-coverage when $c = 4, 5$ than the other methods except SMETANA and NetCoffee. However, as we show later, many of clusters generated by these two methods are not functionally conserved. The total coverage of BEAMS and IsoRank is better than the others because they produce many clusters composed of proteins from 2 or 3 species. These clusters can not explain the data as well as clusters containing proteins from 4 or 5 species can. ConvexAlign has a better CI than all other methods except SMETANA. These conserved interactions may be very helpful in identifying the functional modules conserved among networks of different species. It is worth mentioning that most of the conserved interaction resulting from SMETANA may be spurious [1].

Table 1: Topological evaluation of output clusters by different alignment methods. IsoRankN and BEAMS are tested using three different values of their parameters α.

	IsoRankN (0.3)	IsoRankN (0.5)	IsoRankN (0.7)	SMETANA	NetCoffee	BEAMS (0.3)	BEAMS (0.5)	BEAMS (0.7)	ConvexAlign
c=2	4625 11035	4178 8356	4670 11165	1127 2718	1424 2848	5703 11406	5274 11469	5271 11465	2856 5712
c=3	2259 8521	2270 6810	2304 8750	1653 5808	1739 5217	2192 6576	2557 8128	2556 8118	1833 5499
c=4	1023 5276	731 2924	944 4823	2028 9531	1980 7920	1163 4652	1141 4686	1143 4701	1190 4760
c=5	224 1417	112 560	184 1182	1622 10342	1217 6075	683 3915	600 3046	600 3044	765 3825
Total coverage	8131 26249	7291 18650	8102 25920	6430 28399	6360 22070	9741 26549	9572 27329	9570 27328	6644 19796
CI	0.03	0.02	0.03	0.10	0.03	0.03	0.03	0.03	0.04
CIQ	0.03	0.02	0.02	0.06	0.02	0.02	0.02	0.02	0.03

Biological quality. Table 2 provides the functional consistency measures of the alignments generated by

different methods. The first four multi-rows show the quality of the clusters composed of proteins from $c = 2, 3, 4, 5$ species. In these multi-rows, the top and middle rows show the number of consistent and annotated clusters, respectively, and the bottom row shows specificity. Regardless of c, ConvexAlign outperforms the other methods in terms of specificity and the number of consistent clusters. At the same time, ConvexAlign generates fewer annotated clusters than BEAMS when $c = 2, 3, 4.$, Although SMETANA and NetCoffee generate a larger number of clusters for $c = 4, 5$ than ConvexAlign, their clusters are not very functionally consistent. The fifth row shows ConvexAlign has much higher specificity than the others when all the resulting clusters ($c \geq 2$) are considered. These results suggest that ConvexAlign finds more functionally consistent clusters, not only by generating small clusters (i.e. $c = 2, 3$) but more importantly large clusters (i.e. $c = 4, 5$). These clusters (especially when $c = 4, 5$) are very valuable because they may provide useful information about the orthology relationship among the proteins of all species. Moreover, these clusters can be very useful for identifying conserved sub-networks as well as predicting the function of unannotated proteins. ConvexAlign yields a COI/CI ratio around 60% that is 1.44 times larger than the second best ratio by BEAMS. This result may indicate that ConvexAlign is able to identify conserved interactions between othologous proteins. It also suggests that although SMETANA has the largest CI, many of those conserved interactions are possibly false and formed by non-orthologous proteins. ConvexAlign also outperforms other methods in terms of MNE and sensitivity.

Table 2: Functional consistency of output clusters. Note that for MNE, the smaller the better; while for the other measures, the larger the better.

		IsoRankN (0.3)	IsoRankN (0.5)	IsoRankN (0.7)	SMETANA	NetCoffee	BEAMS (0.3)	BEAMS (0.5)	BEAMS (0.7)	ConvexAlign
c=2	consistent	906	1259	919	295	495	1539	1568	1569	1914
	annotated	3614	2862	3646	931	931	3486	3456	3452	2326
	specifity	0.25	0.44	0.25	0.39	0.53	0.44	0.45	0.45	0.82
c=3	consistent	203	466	231	188	462	1003	1084	1084	1155
	annotated	2160	2153	2210	1556	1640	2119	2442	2441	1741
	specifity	0.09	0.22	0.10	0.12	0.28	0.47	0.44	0.44	0.66
c=4	consistent	41	106	54	170	406	606	624	624	661
	annotated	1020	723	942	2019	1640	1159	1136	1138	1079
	specifity	0.04	0.15	0.06	0.08	0.25	0.52	0.55	0.55	0.61
c=5	consistent	14	19	9	183	406	383	359	359	493
	annotated	224	112	184	1621	1955	683	600	600	763
	specifity	0.06	0.17	0.05	0.11	0.21	0.56	0.60	0.60	0.65
$c \geq 2$	specifity	0.17	0.32	0.17	0.14	0.29	0.48	0.48	0.48	0.71
COI		88	188	127	480	553	1237	1311	1305	1668
COI/CI		0.02	0.13	0.03	0.04	0.21	0.40	0.41	0.41	0.59
MNE		2.15	2.19	2.14	2.44	2.39	1.97	1.95	1.95	1.93
Sensitivity		0.45	0.46	0.45	0.36	0.22	0.33	0.31	0.37	0.51

Table 3 shows the $\overline{AFS}$ separately for clusters composed of proteins in 3, 4, and 5 species in both categories BP and MF. The $\overline{AFS}$ obtained by ConvexAlign is $6 - 20\%$ larger than the other methods. These results indicate that on average the clusters generated by ConvexAlign are functionally more consistent. That is, ConvexAlign outperforms the other methods in terms of not only the number of consistent clusters, but also the average GO semantic similarity. The distribution of AFS scores for clusters composed of proteins in 3, 4, and 5 species is shown in Fig. A.1, in which the middle line in each box shows the median value. That is, the median AFS obtained by ConvexAlign is larger than the other methods. These results further confirm that ConvexAlign yields clusters with higher functional similarity in both categories MF and BP.

Table 3: AFS comparison between ConvexAlign and the other methods

		IsoRankN (0.3)	IsoRankN (0.5)	IsoRankN (0.7)	SMETANA	NetCoffee	BEAMS (0.3)	BEAMS (0.5)	BEAMS (0.7)	ConvexAlign
$\overline{AFS}_{BP}$	c=3	0.83	1.02	0.86	0.74	1.03	1.60	1.63	1.63	**1.74**
	c=4	0.69	0.97	0.72	0.68	0.99	1.63	1.61	1.60	**1.79**
	c=5	0.75	1.01	0.72	0.85	1.16	1.66	1.67	1.67	**1.71**
$\overline{AFS}_{MF}$	c=3	0.80	0.94	0.80	0.69	0.99	1.40	1.33	1.34	**1.54**
	c=4	0.83	1.02	0.86	0.74	1.03	1.60	1.63	1.63	**1.74**
	c=5	0.86	1.06	0.86	0.94	1.18	1.68	1.68	1.68	**1.74**

3.4 Alignment quality on synthetic data

This section explains the results on the NAPAbench benchmark. Fig. 1 shows the number of consistent clusters generated by different methods and their specificity on clusters composed of proteins in $c = 2, 3, 4, 5, 6, 7, 8$ species, respectively. In terms of the number of consistent clusters, ConvexAlign is slightly better than the second best method BEAMS regardless of c, but much better than the others. In terms of specificity, ConvexAlign has a much larger advantage over the other methods when $c = 4, 5, 6, 7$. When $c = 8$, ConveAlign is slightly better than BEAMS, but much better than the others. These results indicate that ConvexAlign aligns proteins in a functionally consistent way, without generating too many spurious clusters in which the proteins appear to be unrelated. Fig. 2 shows that ConvexAlign outperforms all the other methods in terms of both MNE and COI. Due to space limit, the topological evaluation is presented in Fig. A.2.

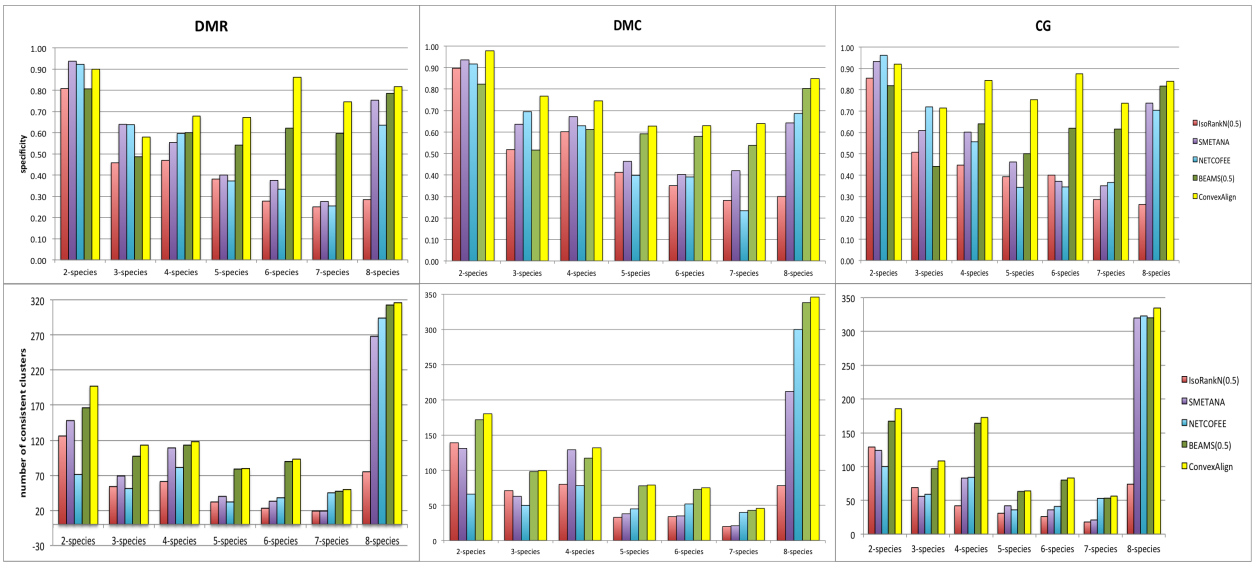

Figure 1: Specificity (top) and the number of consistent clusters (bottom) generated by the competing methods for different c on synthetic data. Only the best performance for IsoRankN and BEAMS is shown.

3.5 Finding conserved subnetworks

One of the applications of network alignment is to reveal subnetworks conserved across the species. These subnetworks may be helpful for extracting biological information that cannot be inferred from sequence similarity alone. Fig. 3 shows one conserved complex detected by ConvexAlign among the 5 species: human,

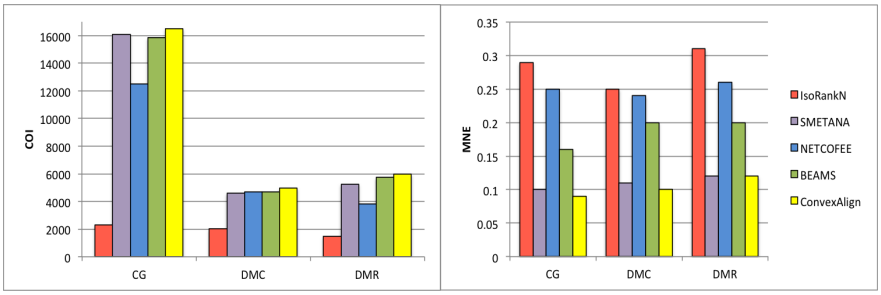

Figure 2: COI and MNE of the clusters generated by the competing methods on synthetic data. Only the best performance for IsoRankN and BEAMS is shown.

yeast, fly, mouse and worm, but not appearing in the alignments generated by other methods. This complex is enriched for proteasome (with p-value$< 10^{-7}$ in all species), which is essential for the degradation of most proteins including misfolded or damaged proteins. The aligned nodes are shown in Table A.1. In Fig. 3, the interactions in IntAct are displayed in solid lines. For fly, mouse and worm, some edges (shown by dotted lines) are missing in IntAct but present in the STRING database [29] with experimental evidence at the highest confidence. Note that our input networks consist of interactions only from IntAct but not STRING. This suggests that ConvexAlign is able to predict missing interactions. We use PANTHER [17] to check if the aligned nodes are orthologous proteins. Most of the aligned proteins are shown to be least divergent orthologs. As shown in Table A.1, there are some missing proteins from different species in some of the clusters. This is because either there are no orthologs in those species or there is no alignment for them. For example, cluster 5 has no proteins from worm and fly. PANTHER could not find any orthologous proteins in those species either. Cluster 6 misses orthologous proteins in fly and yeast, which are aligned by ConvexAlign to proteins not in this proteasome complex. In addition, this proteasome complex has different number of nodes in different species, which implies that ConvexAlign is able to deal with inserted and deleted nodes. Fig. 4 shows another conserved subnetwork detected by ConvexAlign that is related to DNA replication (with p-value$< 6^{-10}$ in all species). Again, this subnetwork cannot be detected by the other methods. PANTHER suggests that the aligned proteins are orthologous and functionally related (see Table A.2).

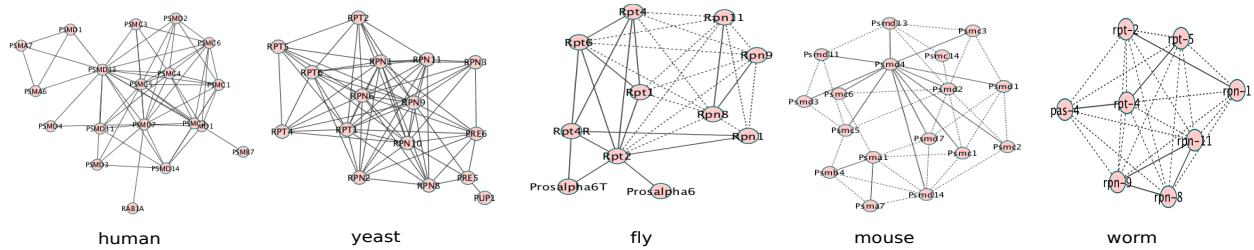

Figure 3: The ConvexAlign-detected proteasome complex in each input PPI network.

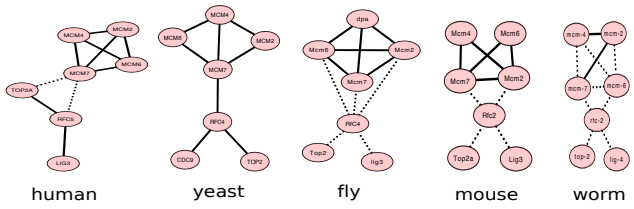

Figure 4: The ConvexAlign-detected DNA replication complex in each input PPI network.

4 Discussion

This paper has presented a new method ConvexAlign for global alignment of multiple PPI networks. ConvexAlign uses a network alignment scoring function that integrates sequence and topological similarity between the matched proteins as well as interaction consistency. Then ConvexAlign uses a novel convex formulation to simultaneously align all the proteins in multiple input networks, resulting in better alignment quality. Such a formulation allows us to use an ADDM method to find its optimal solution.

We have tested ConvexAlign on both real PPI networks and the synthetic data, evaluated the output alignments by different performance metrics and compared it to several popular methods. Experimental results on the real data show that on average ConvexAlign generates more functionally consistent clusters consisting of proteins from most of the input species. That is, ConvexAlign can explain a larger amount of data in a more functionally meaningful way. ConvexAlign can also find a few conserved and biologically important complexes which cannot be detected by the other alignment methods.

In the future we may extend ConvexAlign to produce many-to-many global alignments, which will require some revision of our formulation. It will also be interesting to study how to revise our convex formulation for local alignments of multiple PPI networks. Of course we may also apply ConvexAlign to the alignment of other biological systems such as metabolic networks and protein structures.

Currently the time complexity of our algorithm is $O(M^3K)$, where K is the number iterations in ADMM and M of the total number of proteins. Using a single computer, it takes dozens of hours to align the real PPI networks of the five species and only 1.5 hours to align 8 synthetic networks. The M^3 factor comes from the eigen-decomposition of a $M \times M$ matrix, incurred by the consistency constraint $X \succeq 0$. We may explore a few strategies to speed up this step. For example, we may place the positive semidefinite constraint on a submatrix of X, i.e., enforcing the consistency among only a subset of important nodes (i.e., hub nodes and/or nodes adjacent to hubs). since X is sparse and block-structured, we may also apply some block-based or parallel algorithms to speed up eigen-decomposition.

References

[1] Ferhat Alkan and Cesim Erten. Beams: backbone extraction and merge strategy for the global many-to-many alignment of multiple ppi networks. *Bioinformatics*, 30(4):531–539, 2014. 1, 3, 3.2, 3.3

[2] Giovanni Ciriello, Marco Mina, Pietro H Guzzi, Mario Cannataro, and Concettina Guerra. Alignnemo: a local network alignment method to integrate homology and topology. *PloS one*, 7(6):e38107–e38107, 2012. 1

[3] Jason Flannick, Antal Novak, Chuong B Do, Balaji S Srinivasan, and Serafim Batzoglou. Automatic parameter learning for multiple network alignment. In *Research in Computational Molecular Biology*, pages 214–231. Springer, 2008. 1

[4] Vladimir Gligorijevic, Noël Malod-Dognin, and Nata?a Pržulj. Fuse: multiple network alignment via data fusion. *arXiv:1410.7585 [q-bio.MN]*, 2014. 1

[5] Somaye Hashemifar and Jinbo Xu. Hubalign: an accurate and efficient method for global alignment of protein–protein interaction networks. *Bioinformatics*, 30(17):i438–i444, 2014. 1, 2.1

[6] Jialu Hu, Birte Kehr, and Knut Reinert. Netcoffee: a fast and accurate global alignment approach to identify functionally conserved proteins in multiple networks. *Bioinformatics*, page btt715, 2013. 1, 3, 3.2

[7] Qi-Xing Huang and Leonidas Guibas. Consistent shape maps via semidefinite programming. In *Proceedings of the Eleventh Eurographics/ACMSIGGRAPH Symposium on Geometry Processing*, SGP '13, pages 177–186, Aire-la-Ville, Switzerland, Switzerland, 2013. Eurographics Association. 2.2

[8] Qixing Huang, Vladlen Koltun, and Leonidas Guibas. Joint shape segmentation with linear programming. *ACM Trans. Graph.*, 30(6):125:1–125:12, December 2011. 2.2

[9] Maxim Kalaev, Mike Smoot, Trey Ideker, and Roded Sharan. Networkblast: comparative analysis of protein networks. *Bioinformatics*, 24(4):594–596, 2008. 1

[10] Samuel Kerrien, Bruno Aranda, Lionel Breuza, Alan Bridge, Fiona Broackes-Carter, Carol Chen, Margaret Duesbury, Marine Dumousseau, Marc Feuermann, Ursula Hinz, et al. The intact molecular interaction database in 2012. *Nucleic acids research*, page gkr1088, 2011. 3.1

[11] Wan Kyu Kim and Edward M Marcotte. Age-dependent evolution of the yeast protein interaction network suggests a limited role of gene duplication and divergence. *PLoS Comput Biol*, 4(11):e1000232, 2008. 3.1

[12] Mehmet Koyutürk, Yohan Kim, Umut Topkara, Shankar Subramaniam, Wojciech Szpankowski, and Ananth Grama. Pairwise alignment of protein interaction networks. *Journal of Computational Biology*, 13(2):182–199, 2006. 1

[13] Oleksii Kuchaiev and Nataša Pržulj. Integrative network alignment reveals large regions of global network similarity in yeast and human. *Bioinformatics*, 27(10):1390–1396, 2011. 1

[14] M. Pawan Kumar, Vladimir Kolmogorov, and Philip H. S. Torr. An analysis of convex relaxations for map estimation of discrete mrfs. *JOURNAL OF MACHINE LEARNING RESEARCH*, 10:71–106, 2008. 2.2

[15] Chung-Shou Liao, Kanghao Lu, Michael Baym, Rohit Singh, and Bonnie Berger. Isorankn: spectral methods for global alignment of multiple protein networks. *Bioinformatics*, 25(12):i253–i258, 2009. 1, 3

[16] Noël Malod-Dognin and Nataša Pržulj. L-graal: Lagrangian graphlet-based network aligner. *Bioinformatics*, page btv130, 2015. 2.1

[17] Huaiyu Mi, Qing Dong, Anushya Muruganujan, Pascale Gaudet, Suzanna Lewis, and Paul D Thomas. Panther version 7: improved phylogenetic trees, orthologs and collaboration with the gene ontology consortium. *Nucleic acids research*, 38(suppl 1):D204–D210, 2010. 3.5

[18] Behnam Neyshabur, Ahmadreza Khadem, Somaye Hashemifar, and Seyed Shahriar Arab. Netal: a new graph-based method for global alignment of protein–protein interaction networks. *Bioinformatics*, 29(13):1654–1662, 2013. 1

[19] Rob Patro and Carl Kingsford. Global network alignment using multiscale spectral signatures. *Bioinformatics*, 28(23):3105–3114, 2012. 1

[20] Catia Pesquita, Daniel Faria, Andre O Falcao, Phillip Lord, and Francisco M Couto. Semantic similarity in biomedical ontologies. *PLoS Comput Biol*, 5(7):e1000443, 2009. 3.2

[21] Sayed Mohammad Ebrahim Sahraeian and Byung-Jun Yoon. A network synthesis model for generating protein interaction network families. *PloS one*, 7(8):e41474, 2012. 3.1

[22] Sayed Mohammad Ebrahim Sahraeian and Byung-Jun Yoon. Smetana: accurate and scalable algorithm for probabilistic alignment of large-scale biological networks. *PLoS One*, 8(7):e67995, 2013. 1, 3

[23] Vikram Saraph and Tijana Milenković. Magna: Maximizing accuracy in global network alignment. *Bioinformatics*, 30(20):2931–2940, 2014. 1

[24] Andreas Schlicker, Francisco S Domingues, Jörg Rahnenführer, and Thomas Lengauer. A new measure for functional similarity of gene products based on gene ontology. *BMC bioinformatics*, 7(1):302, 2006. 3.2

[25] Roded Sharan, Silpa Suthram, Ryan M Kelley, Tanja Kuhn, Scott McCuine, Peter Uetz, Taylor Sittler, Richard M Karp, and Trey Ideker. Conserved patterns of protein interaction in multiple species. *Proceedings of the National Academy of Sciences of the United States of America*, 102(6):1974–1979, 2005. 1

[26] Rohit Singh, Jinbo Xu, and Bonnie Berger. Pairwise global alignment of protein interaction networks by matching neighborhood topology. In *Research in computational molecular biology*, pages 16–31. Springer, 2007. 1

[27] Rohit Singh, Jinbo Xu, and Bonnie Berger. Global alignment of multiple protein interaction networks with application to functional orthology detection. *Proceedings of the National Academy of Sciences*, 105(35):12763–12768, 2008. 1

[28] Ricard V Solé, Romualdo Pastor-Satorras, Eric Smith, and Thomas B Kepler. A model of large-scale proteome evolution. *Advances in Complex Systems*, 5(01):43–54, 2002. 3.1

[29] Damian Szklarczyk, Andrea Franceschini, Michael Kuhn, Milan Simonovic, Alexander Roth, Pablo Minguez, Tobias Doerks, Manuel Stark, Jean Muller, Peer Bork, et al. The string database in 2011: functional interaction networks of proteins, globally integrated and scored. *Nucleic acids research*, 39(suppl 1):D561–D568, 2011. 3.5

[30] Andrei Todor, Alin Dobra, and Tamer Kahveci. Probabilistic biological network alignment. *IEEE/ACM Transactions on Computational Biology and Bioinformatics (TCBB)*, 10(1):109–121, 2013. 1

[31] Alexei Vázquez, Alessandro Flammini, Amos Maritan, and Alessandro Vespignani. Modeling of protein interaction networks. *Complexus*, 1(1):38–44, 2003. 3.1

[32] V Vijayan, V Saraph, and T Milenković. Magna++: Maximizing accuracy in global network alignment via both node and edge conservation. *Bioinformatics*, page btv161, 2015. 1

APPENDIX

A Results

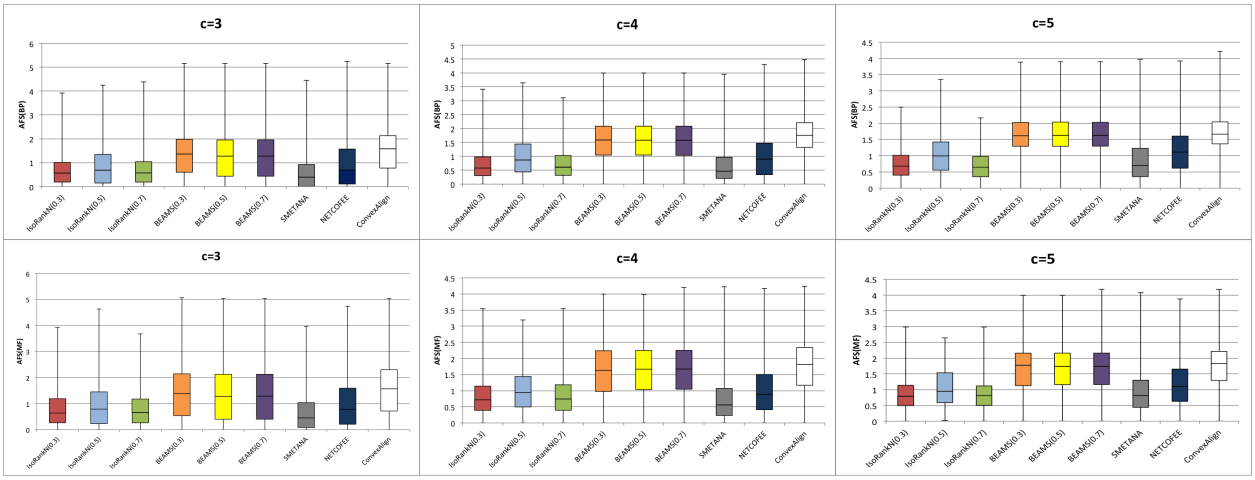

Figure A.1: AFS distribution resulting from different methods on real data.

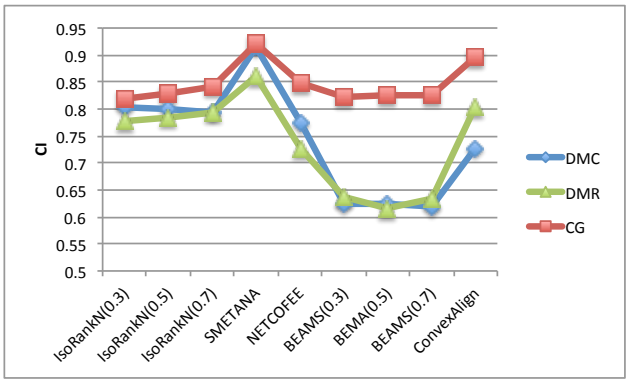

Figure A.2: CI analysis on synthetic data.

B Schlicker's similarity

Given two GO terms g_1, g_2 and their least common ancestor g_c, the Resnik ontological similarity is defined as $sim_Resnik(g_1, g_2) = IC(g_c)$, where $IC(g)$ is the information content of the term g in the given annotation dataset. Considering two gene products p and q annotated with the sets GO^p and GO^q of GO terms, respectively with sizes N and M, a similarity matrix S is calculated such as:

$$s_{ij} = sim_{Resnik}(GO_i^p, GO_j^q), \forall i \in \{1, \cdots, N\}, \forall j \in \{1, \cdots, M\}$$

This matrix contains all pairwise similarity values between all GO terms associated to p and q. The average over the row maxima and the column maxima, respectively, gives similarity values for the comparison of p

Table A.1: Clusters of aligned nodes that are enriched for proteasome.

	mouse	worm	yeast	fly	human
cluster 1	Psmb4	-	PUP1	-	PSMB7
cluster 2	Psmd7	rpn-8	RPN8	Rpn8	PSMD7
cluster 3	Psma1	-	PRE5	Prosalpha6T	PSMA6
cluster 4	Psmd14	rpn-11	RPN11	Rpn11	PSMD14
cluster 5	Psmd1	-	RPN2	-	PSMD1
cluster 6	Rab1A	-	-	-	RAB1A
cluster 7	Psmc6	rpt-4	RPT4	Rpt4	PSMC6
cluster 8	Psmc3	rpt-5	RPT5	Rpt4R	PSMC3
cluster 9	Psmd2	rpn-1	RPN1	Rpn1	PSMD2
cluster 10	Psma7	pas-4	PRE6	Prosalpha6	PSMA7
cluster 11	Psmc2	-	RPT1	Rpt1	PSMC2
cluster 12	Psmc1	rpt-2	RPT2	Rpt2	PSMC1
cluster 13	Psmc5	-	RPT6	Rpt6	PSMC5
cluster 14	Psmd13	rpn-9	RPN9	Rpn9	PSMD13
cluster 15	Psmd11	-	RPN6	-	PSMD11
cluster 16	Psmd3	-	RPN3	-	PSMD3
cluster 17	Psmd4	-	RPN10	-	PSMD4

Table A.2: Clusters of aligned nodes that are enriched for DNA replication.

	mouse	worm	yeast	fly	human
cluster 1	Top2a	top-2	CDC25C	Top2	TOP2A
cluster 2	Mcm2	mcm-2	MCM2	Mcm2	MCM2
cluster 3	Mcm4	mcm-4	MCM4	dpa	MCM4
cluster 4	Mcm6	mcm-6	MCM6	Mcm6	MCM6
cluster 5	Mcm7	mcm-7	MCM7	Mcm7	MCM7
cluster 6	Lig3	lig-4	CDC9	lig3	LIG3
cluster 7	Rfc2	rfc-2	RFC4	RfC4	RFC5

to q and the comparison of q to p:

$$score_{row} = \frac{1}{N}\sum_{(i=1)}^{N} max(s_{ij})_{(1\leq j\leq M)}, score_{column} = \frac{1}{M}\sum_{(j=1)}^{M} max(s_{ij})_{(1\leq i\leq N)}.$$

The Schlicker's similarity is then calculated as $sim_{func}(p,q) = max\{score_{row}, score_{column}\}$.

C Parameter selection

For all the experiments in this paper, we set the parameters as $\lambda_1 = 0.3$, and $\lambda_2 = 0.02$. These parameters are chosen via 10-fold cross-validation in optimizing the GO-term scores of the alignment between the mouse and worm networks. The weight factor for aligned interactions is small because: 1) there are many more aligned interactions than aligned nodes, so a small λ_2 may place the node and interaction scores at the similar scale; and 2) the topological score used in our scoring function already encodes some interaction information and thus, may overlap with the interaction score. Of course we may increase λ_2 to favor other performance metrics such as the number of aligned interactions and the number of annotated clusters.

D Proof of Proposition 1

Proof. Let V_i be a vertex set corresponding to all rows in the block X_{ii}. Then X_{ii} has size $|V_i| \times V_i$. Each block X_{ij} has size $|V_i| \times |V_j|$, describing the relationship between V_i and V_j. Let $V = \cup_{1 \le i \le N} V_i$, then the binary block matrix X has size $|V| \times |V|$. Ignoring the N blocks X_{ii} ($1 \le i \le N$), the binary block matrix X can be treated as an adjacency matrix of a simple graph $\mathcal{M}$. That is, starting from X, we may construct a simple graph $\mathcal{M}$ for V such that one non-zero entry in X corresponds to one edge in $\mathcal{M}$.

According to the constraints $X_{ij}\mathbf{1} \le \mathbf{1}, X_{ij}^T\mathbf{1} \le \mathbf{1}$, it is easy to see that each connected component of $\mathcal{M}$ contains at most one vertex from each V_i. Now we want to prove that each connected component in $\mathcal{M}$ is a clique. This is equivalent to proving the consistency property, i.e., given three vertices $v_i \in V_i, v_j \in V_j, v_k \in V_k$, if $X_{ij}(v_i, v_j) = X_{ik}(v_i, v_k) = 1$, then $X_{jk}(v_j, v_k) = 1$. This can be induced from that X is positive semidefinite. Consider the 3×3 principal submatrix of X induced by v_i, v_j, v_k. Since the principle submatrix of a positive semidefinite matrix is also semidefinite positive, we have

$$\begin{pmatrix} 1 & 1 & 1 \\ 1 & 1 & X_{jk}(v_j, v_k) \\ 1 & X_{jk}(v_j, v_k) & 1 \end{pmatrix} \succeq 0.$$

It follows that

$$det(\begin{pmatrix} 1 & 1 & 1 \\ 1 & 1 & X_{jk}(v_j, v_k) \\ 1 & X_{jk}(v_j, v_k) & 1 \end{pmatrix}) = -(1 - X_{jk}(v_j, v_k))^2.$$

This implies $X_{jk}(v_j, v_k) = 1$.

Let $\mathcal{A} = \{A_1, A_2, ..., A_K\}$ denote all the connected components of $\mathcal{M}$. Then $\mathcal{A}$ is a feasible one-to-one alignment between the N vertex sets V_1,V_2,...,V_N. For each vertex V_i, we construct a binary matrix Y_i of size $|V_i| \times K$. For any k ($1 \le k \le K$) and $v_i \in V_i$, if v_i appears in A_k, then $Y_i(v_i, k) = 1$; otherwise $Y_i(v_i, k) = 0$. Finally we construct a $|V| \times K$ binary matrix Y by stacking Y_1, Y_2,...,Y_N along the vertical direction. It is easy to show that $X = YY^T$. □

E Optimization via ADMM (Alternating Direction Method of Multipliers)

In this section, we describe in detail how to solve the optimization problem in (13) using ADMM. The basic idea is to augment its Lagrangian dual (see ??) and iteratively optimize a subset of variables while keeping the others fixed. This allows us to exploit structure patterns in the constraint set for effective optimization. To maximize the power of ADMM, we introduce a latent variable $\boldsymbol{s}_{ij}$ to break each constraint $B_{ij}\boldsymbol{y}_{ij} \le \mathcal{F}_{ij}(X_{ij})$ into two sets of constraints $B_{ij}\boldsymbol{y}_{ij} \le \boldsymbol{s}_{ij}$ and $\boldsymbol{s}_{ij} = \mathcal{F}_{ij}(X_{ij})$. Let $\lambda = \frac{\lambda_2}{1-\lambda_2}$ and $\boldsymbol{d}_{ij}$ be

the coefficient of $\boldsymbol{y}_{ij}$. The relaxed convex optimization problem can be written as follows.

$$
\begin{aligned}
\text{maximize} \quad & \sum_{1\le i<j\le N} \Big(\langle C_{ij}, X_{ij}\rangle + \lambda \langle \mathbf{d}_{ij}, \mathbf{y}_{ij}\rangle \Big) \\
\text{subject to} \quad & \boldsymbol{y}_{ij} \ge \mathbf{0},\ 1 \le i \le j \le N && : \boldsymbol{z}^0_{ij} \ge 0 \\
& B_{ij}\boldsymbol{y}_{ij} \le \boldsymbol{s}_{ij},\ 1 \le i \le j \le N && : \boldsymbol{z}_{ij,1} \ge 0 \\
& \boldsymbol{s}_{ij} = \mathcal{F}_{ij}(X_{ij}),\ 1 \le i < j \le N && : \boldsymbol{z}_{ij,2} \\
& X_{ij}\mathbf{1} \le \mathbf{1},\ 1 \le i \le j \le N && : \boldsymbol{z}_{ij,3} \ge 0 \\
& X_{ij}^T\mathbf{1} \le \mathbf{1},\ 1 \le i \le j \le N && : \boldsymbol{z}_{ij,4} \ge 0 \\
& X_{ij} \ge 0,\ 1 \le i \le j \le N && : Z_{ij,5} \ge 0 \\
& X_{ii} = I_{|V_i|},\ 1 \le i \le N && : Z_{ii,6} \\
& X \succeq 0 && : S \succeq 0
\end{aligned} \tag{14}
$$

Note that the right column shows the dual variables of the corresponding constraints. Using the dual variables, the Lagrangian of the above problem is as follows:

$$
\begin{aligned}
\mathcal{L} = & \sum_{1\le i<j\le N} \Big(- \langle C_{ij}, X_{ij}\rangle - \lambda\langle \boldsymbol{d}_{ij}, \boldsymbol{y}_{ij}\rangle - \langle \boldsymbol{z}_{ij,0}, \boldsymbol{y}_{ij}\rangle + \langle \boldsymbol{z}_{ij,1}, B_{ij}\boldsymbol{y}_{ij} - \boldsymbol{s}_{ij}\rangle + \langle \boldsymbol{z}_{ij,2}, \boldsymbol{s}_{ij} - \mathcal{F}_{ij}(X_{ij})\rangle \\
& \qquad + \langle \boldsymbol{z}_{ij,3}, X\mathbf{1} + \mathbf{1}\rangle + \langle \boldsymbol{z}_{ij,4}, X^T\mathbf{1} - \mathbf{1}\rangle - \langle Z_{ij,5}, X_{ij}\rangle - 2\langle S_{ij}, X_{ij}\rangle \Big) \\
& + \sum_{1\le i\le N} \Big(\langle Z_{ii,6}, X_{ii} - I_{|V_i|}\rangle - \langle S_{ii}, X_{ii}\rangle \Big) \\
= & \sum_{1\le i<j\le N} \Big(- \langle \mathbf{1}, \boldsymbol{z}_{ij,3}\rangle - \langle \mathbf{1}, \boldsymbol{z}_{ij,4}\rangle - \langle C_{ij} + \mathcal{F}_{ij}^T(\boldsymbol{z}_{ij,2}) - \boldsymbol{z}_{ij,3}\mathbf{1}^T - \mathbf{1}\boldsymbol{z}_{ij,4}^T + Z_{ij,5}, X_{ij}\rangle \\
& \quad - \langle \lambda\boldsymbol{d}_{ij} + \boldsymbol{z}_{ij,0} - B_{ij}^T\boldsymbol{z}_{ij,1}, \boldsymbol{y}_{ij}\rangle - \langle \boldsymbol{z}_{ij,1} - \boldsymbol{z}_{ij,2}, \boldsymbol{s}_{ij}\rangle \Big) \\
& + \sum_{1\le i\le N} \Big(- \langle I_{|V_i|}, Z_{ii,6}\rangle - \langle S_{ii} - Z_{ii,6}, X_{ii}\rangle \Big).
\end{aligned} \tag{15}
$$

The augmented Lagrangian dual of the above problem is as follows.

$$
\begin{aligned}
\mathcal{L}' = & \sum_{1\le i<j\le N} \Big(\langle \mathbf{1}, \boldsymbol{z}_{ij,3}\rangle - \langle \mathbf{1}, \boldsymbol{z}_{ij,4}\rangle + \langle C_{ij} + \mathcal{F}_{ij}^T(\boldsymbol{z}_{ij,2}) - \boldsymbol{z}_{ij,3}\mathbf{1}^T - \mathbf{1}\boldsymbol{z}_{ij,4}^T + Z_{ij,5} + 2S_{ij}, X_{ij}\rangle \\
& \quad + \langle \lambda\boldsymbol{d}_{ij} + \boldsymbol{z}_{ij,0} - B_{ij}^T\boldsymbol{z}_{ij,1}, \boldsymbol{y}_{ij}\rangle + \langle \boldsymbol{z}_{ij,1} - \boldsymbol{z}_{ij,2}, \boldsymbol{s}_{ij}\rangle \\
& \quad + \frac{1}{2\mu}\big(\|C_{ij} + \mathcal{F}_{ij}^T(\boldsymbol{z}_{ij,2}) - \boldsymbol{z}_{ij,3}\mathbf{1}^T - \mathbf{1}\boldsymbol{z}_{ij,4}^T + Z_{ij,5} + 2S_{ij}\|_F^2 + \|\lambda\boldsymbol{d}_{ij} + \boldsymbol{z}_{ij,0} - B_{ij}^T\boldsymbol{z}_{ij,1}\|^2 + \|\boldsymbol{z}_{ij,1} - \boldsymbol{z}_{ij,2}\|^2 \big) \Big) \\
& + \sum_{1\le i\le N} \Big(\langle I_{|V_i|}, Z_{ii,6}\rangle + \langle S_{ii} - Z_{ii,6}, X_{ii}\rangle + \frac{1}{2\mu}\|S_{ii} - Z_{ii,6}\|_F^2 \Big).
\end{aligned} \tag{16}
$$

$\mathcal{L}'$ shall be maximized with respect to the primal variables but minimized with respect to the dual variables. We initialize all the primal and dual variables to zero. At iteration $k+1$, we update the dual and primal variables as follows.

Step 1: Optimizing $\boldsymbol{z}_{ij,0}^{(k+1)}$. When variable $\boldsymbol{z}_{ij,0}$ is active with other variables fixed, the optimization problem is equivalent to computing

$$
\min_{\boldsymbol{z}_{ij,0}\ge 0} \|\lambda\boldsymbol{d}_{ij} + \boldsymbol{z}_{ij,0} - B_{ij}^T\boldsymbol{z}_{ij,1}^{(k)} + \mu\boldsymbol{y}_{ij}^{(k)}\|^2, \quad 1 \le i < j \le N
$$

In this case, we have

$$\boldsymbol{z}_{ij,0}^{(k+1)} = \max(0, B_{ij}^T \boldsymbol{z}_{ij,1}^{(k)} - \mu \boldsymbol{y}_{ij}^{(k)} - \lambda \boldsymbol{d}_{ij}), \quad 1 \leq i < j \leq N$$

Step 2: Optimizing $\boldsymbol{z}_{ij,1}^{(k+1)}$. When $\boldsymbol{z}_{ij,1}$ is active while other variables are fixed, each of them can be optimized independently as

$$\min_{\boldsymbol{z}_{ij,1} \geq 0} \|B_{ij}^T \boldsymbol{z}_{ij,1} - \Big(\lambda \boldsymbol{d}_{ij} + \boldsymbol{z}_{ij,0}^{(k+1)} + \mu \boldsymbol{y}_{ij}^{(k)}\Big)\|^2 + \|\boldsymbol{z}_{ij,1} - \boldsymbol{z}_{ij,2}^{(k)}\|^2.$$

Since each $\boldsymbol{y}$ appears in 4 constraints of (10), we permute the rows of B_{ij} to form 4 submatrices $B_{ij,1}, B_{ij,2}, B_{ij,3}, B_{ij,4}$, so that each column of one submatrix contains exactly one non-zero entry. Accordingly, we can also reorder and rewrite $\boldsymbol{z}_{ij,1}$ as $(\boldsymbol{z}_{ij,1,1}; \boldsymbol{z}_{ij,1,2}; \boldsymbol{z}_{ij,1,3}; \boldsymbol{z}_{ij,1,4})$. Then we alternate the optimization of $\boldsymbol{z}_{ij,1,l} (l = 1, 2, 3, 4)$ as follows.

$$\boldsymbol{z}_{ij,1,l}^{(k+1)} = \arg \min_{\boldsymbol{z}_{ij,1,l} \geq 0} \|B_{ij,l}^T \boldsymbol{z}_{ij,1,l} - \Big(\lambda \boldsymbol{d}_{ij} + \boldsymbol{z}_{ij,0}^{(k+1)} + \mu \boldsymbol{y}_{ij}^{(k)} - \sum_{p \neq l} B_{ij,p}^T \boldsymbol{z}_{ij,1,p}^{\star}\Big)\|^2 + \|\boldsymbol{z}_{ij,1,l} - \boldsymbol{z}_{ij,2,l}^{(k)}\|^2. \tag{17}$$

where $\boldsymbol{z}_{ij,1,p}^{\star}$ is the latest value of $\boldsymbol{z}_{ij,1,p}$. Due to the special structure of $B_{ij,l} (l = 1, 2, 3, 4)$, the elements of $\boldsymbol{z}_{ij,1,l}$ can be optimized independently, leading to explicit expressions of optimal values:

$$\boldsymbol{z}_{ij,1,l}^{(k+1)} = \max\big(0, (B_{ij,l} B_{ij,l}^T + I)^{-1} (B_{ij,l} (\lambda \boldsymbol{d}_{ij} + \boldsymbol{z}_{ij,0}^{(k+1)} + \mu \boldsymbol{y}_{ij}^{(k)} - \sum_{p \neq l} B_{ij,p}^T \boldsymbol{z}_{ij,1,p}^{\star}) + \boldsymbol{z}_{ij,2,l}^{(k)})\big).$$

where $B_{ij,l} B_{ij,l}^T + I$ is a diagonal matrix and $\boldsymbol{z}_{ij,1,p}^{\star}$ is the latest value of $\boldsymbol{z}_{ij,1,p}$.

Step 3: Optimizing $\boldsymbol{z}_{ij,2}^{(k+1)}$, $\boldsymbol{z}_{ij,3}$, $\boldsymbol{z}_{ij,4}$, $Z_{ij,5}$ and $Z_{ii,6}$. The optimization of each $\boldsymbol{z}_{ij,2}$ is decoupled and its optimal value is

$$\begin{aligned}
\boldsymbol{z}_{ij,2}^{(k+1)} &= \arg \min_{\boldsymbol{z}_{ij,2}} \|\mathcal{F}^T(\boldsymbol{z}_{ij,2}) - \Big(\boldsymbol{z}_{ij,3}^{(k)} \mathbf{1}^T + \mathbf{1} {\boldsymbol{z}_{ij,4}^{(k)}}^T - C - Z_{ij,5}^{(k)} - 2S_{ij}^{(k)} - \mu X_{ij}^{(k)}\Big)\|_F^2 + \|\boldsymbol{z}_{ij,2} - \boldsymbol{z}_{ij,1}^{(k+1)}\|^2 \\
&= (\mathcal{F}\mathcal{F}^T + I)^{-1} \Big(\mathcal{F}\big(\boldsymbol{z}_{ij,3}^{(k)} \mathbf{1}^T + \mathbf{1} {\boldsymbol{z}_{ij,4}^{(k)}}^T - C - Z_{ij,5}^{(k)} - 2S_{ij}^{(k)} - \mu X_{ij}^{(k)}\big) + \boldsymbol{z}_{ij,1}^{(k+1)}\Big).
\end{aligned} \tag{18}$$

where $\mathcal{F}\mathcal{F}^T + I$ is a diagonal matrix. Through a similar derivation, we can compute the optimal value of other variables at iteration $k+1$ as

$$\begin{aligned}
\boldsymbol{z}_{ij,3}^{(k+1)} &= \arg \min_{\boldsymbol{z}_{ij,3} \geq 0} \|\boldsymbol{z}_{ij,3} \mathbf{1}^T - \Big(C_{ij} + \mathcal{F}^T(\boldsymbol{z}_{ij,2}^{(k+1)}) + Z_{ij,5}^{(k)} + \mu X_{ij}^{(k)} - \mathbf{1} {\boldsymbol{z}_{ij,4}}^{(k)}\Big)\|_F^2 + 2\mu \langle \mathbf{1}, \boldsymbol{z}_{ij,3} \rangle \\
&= \max(0, \Big(\big(C_{ij} + \mathcal{F}^T(\boldsymbol{z}_{ij,2}^{(k+1)}) + Z_{ij,5}^{(k)} + \mu X_{ij}^{(k)} - \mathbf{1} {\boldsymbol{z}_{ij,4}}^{(k)}\big)\mathbf{1} - \mu\Big)/|V_j|)
\end{aligned} \tag{19}$$

$$\begin{aligned}
\boldsymbol{z}_{ij,4}^{(k+1)} &= \arg \min_{\boldsymbol{z}_{ij,4} \geq 0} \|\mathbf{1} \boldsymbol{z}_{ij,4}^T - \Big(C_{ij} + \mathcal{F}^T(\boldsymbol{z}_{ij,2}^{(k+1)}) + Z_{ij,5}^{(k)} + \mu X_{ij}^{(k)} - {\boldsymbol{z}_{ij,3}}^{(k+1)} \mathbf{1}^T\Big)\|_F^2 + 2\mu \langle \mathbf{1}, \boldsymbol{z}_{ij,4} \rangle \\
&= \max(0, \Big(\big(C_{ij} + \mathcal{F}^T(\boldsymbol{z}_{ij,2}^{(k+1)}) + Z_{ij,5}^{(k)} + \mu X_{ij}^{(k)} - \mathbf{1} {\boldsymbol{z}_{ij,4}}^{(k)}\big)^T \mathbf{1} - \mu\Big)/|V_i|)
\end{aligned} \tag{20}$$

$$
\begin{aligned}
Z_{ij,5}^{(k+1)} &= \arg\min_{Z_{ij,5}\geq 0} \|Z_{ij,5} - \Big(\boldsymbol{z}_{ij,3}^{(k+1)}\mathbf{1}^T + \mathbf{1}\boldsymbol{z}_{ij,4}^{(k+1)^T} - C_{ij} - \mathcal{F}_2^T(\boldsymbol{z}_{ij,2}^{(k+1)}) - \mu X_{ij}^{(k)} - 2S_{ij}^{(k)}\Big)\|_F^2 \\
&= \max\Big(0, \boldsymbol{z}_{ij,3}^{(k+1)}\mathbf{1}^T + \mathbf{1}\boldsymbol{z}_{ij,4}^{(k+1)^T} - C_{ij} - \mathcal{F}_2^T(\boldsymbol{z}_{ij,2}^{(k+1)}) - \mu X_{ij}^{(k)} - 2S_{ij}^{(k)}\Big), \\
Z_{ii,6}^{(k+1)} &= \arg\min_{Z_{ii,6}\geq 0} \|S_{ii} + \mu X_{ii} - Z_{ii,6} - \mu I_{|V_i|}\|_F^2 \\
&= \max\Big(0, S_{ii}^{(k)} + \mu X_{ii}^{(k)} - \mu I_{|V_i|}\Big).
\end{aligned} \tag{21}
$$

Step 4: Optimizing S. Finally, we optimize S. In this case, the optimization problem is reduced to

$$
\begin{aligned}
S^{(k+1)} &= \arg\min_{S\geq 0} \sum_{1\leq i<j\leq N} \|C_{ij} + \mathcal{F}_{ij}^T(\boldsymbol{z}_{ij,2}^{(k+1)}) - \boldsymbol{z}_{ij,3}^{(k+1)}\mathbf{1}^T - \mathbf{1}\boldsymbol{z}_{ij,4}^{(k+1)^T} + Z_{ij,5}^{(k+1)} + 2S_{ij} + \mu X_{ij}^{(k)}\|_F^2 \\
&\quad + \sum_{1\leq i\leq N} \|S_{ii} - Z_{ii,6}^{(k+1)} + \mu X_{ii}^{(k)}\| \qquad (22) \\
&= \arg\min_{S\geq 0} \|S - T^{(k)}\|_F^2 \\
&= U\max(\Sigma, 0)U^T, \qquad (23)
\end{aligned}
$$

where $U\Sigma U^T$ is eigen-decomposition of $T^{(k)}$ defined below and $\max(\Sigma, 0)$ takes the positive eigenvalues.

$$
T_{ij}^{(k+1)} = \begin{cases} \Big(\boldsymbol{z}_{ij,3}^{(k+1)}\mathbf{1}^T + \mathbf{1}\boldsymbol{z}_{ij,4}^{(k+1)^T} - C_{ij} - F_{ij}^T(\boldsymbol{z}_{ij,2}^{(k+1)} - \mu X_{ij}^{(k)}\Big)/2 & i \neq j \\ Z_{ii,6}^{(k+1)} - \mu X_{ii}^{(k)} & \text{otherwise} \end{cases} \tag{24}
$$

Step 5: Optimizing primal variables. Finally the primal variables are updated as follows:

$$
\begin{aligned}
\boldsymbol{y}_{ij}^{(k+1)} &= \boldsymbol{y}_{ij}^{(k)} + \frac{1}{\mu}\Big(\lambda\mathbf{1} + \boldsymbol{z}_{ij,0}^{(k+1)} - B^T\boldsymbol{z}_{ij,1}^{(k+1)}\Big), \\
X_{ij}^{(k+1)} &= X_{ij}^{(k)} + \frac{1}{\mu}\Big(C_{ij} + \mathcal{F}_{ij}^T(\boldsymbol{z}_{ij,2}^{(k+1)}) - \boldsymbol{z}_{ij,3}^{(k+1)}\mathbf{1}^T - \mathbf{1}\boldsymbol{z}_{ij,4}^{(k+1)^T} + Z_{ij,5}^{(k+1)} + 2S_{ij}^{(k+1)}\Big) \\
\boldsymbol{s}^{(k+1)} &= \boldsymbol{s}^{(k)} + \frac{1}{\mu}(\boldsymbol{z}_1^{(k+1)} - \boldsymbol{z}_2^{(k+1)}).
\end{aligned} \tag{25}
$$